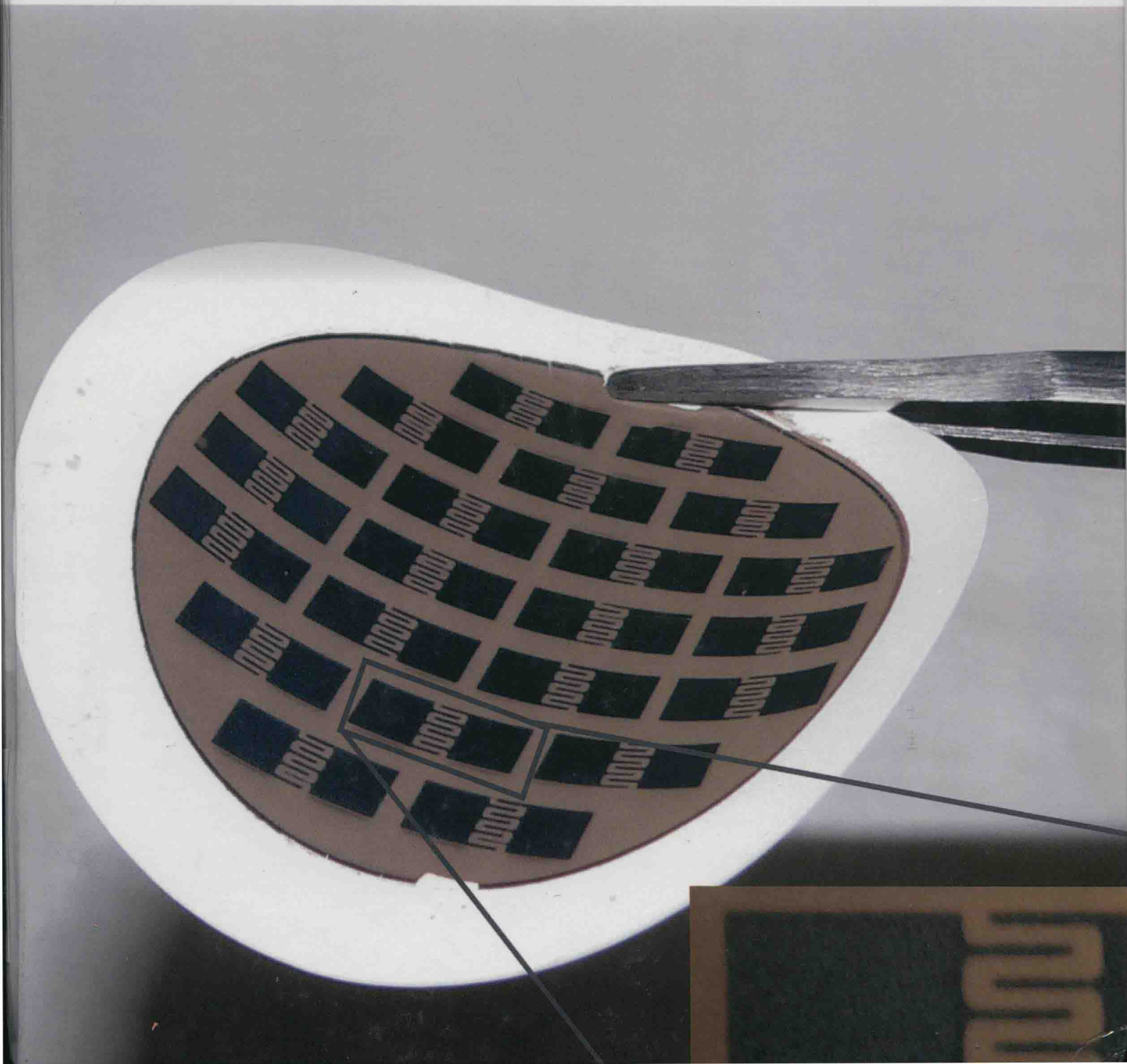


# Recent Developments in **Nanomaterials**

**Andrew Green**

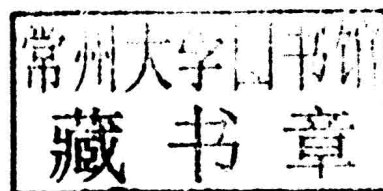
**Volume III**



# Recent Developments in Nanomaterials

## Volume III

Edited by **Andrew Green**



**NY**RESEARCH  
P R E S S

New York

Published by NY Research Press,  
23 West, 55th Street, Suite 816,  
New York, NY 10019, USA  
[www.nyresearchpress.com](http://www.nyresearchpress.com)

**Recent Developments in Nanomaterials: Volume III**  
Edited by Andrew Green

© 2015 NY Research Press

International Standard Book Number: 978-1-63238-393-8 (Hardback)

This book contains information obtained from authentic and highly regarded sources. Copyright for all individual chapters remain with the respective authors as indicated. A wide variety of references are listed. Permission and sources are indicated; for detailed attributions, please refer to the permissions page. Reasonable efforts have been made to publish reliable data and information, but the authors, editors and publisher cannot assume any responsibility for the validity of all materials or the consequences of their use.

The publisher's policy is to use permanent paper from mills that operate a sustainable forestry policy. Furthermore, the publisher ensures that the text paper and cover boards used have met acceptable environmental accreditation standards.

**Trademark Notice:** Registered trademark of products or corporate names are used only for explanation and identification without intent to infringe.

Printed in China.

# **Recent Developments in Nanomaterials**

## **Volume III**



## Preface

When a chemical substance or material is manufactured and utilized in any application at a very small scale, we call it nanomaterial. They can be 10,000 times smaller than the diameter of human hair. Nanomaterials exhibit characteristics such as conductivity, chemical reactivity and increased strength in comparison to the material without nanoscale feature.

Applications of Nanomaterials are already in use such as batteries, anti bacterial clothing, coating etc. By the end of 2015 it is being expected that the market will grow to hundreds of billions. It is also being expected that the sectors like health, industry, innovation, environment, energy, transport, information society, employment and occupational safety and health, security and space will be flooded by nano innovations.

Nanomaterials are also believed to have the potential that will improve the quality and also they can contribute in industrial competitiveness. However, everything comes with pros and cons and these nanomaterials can pose risks to human life, but with existing risk assessment measures; it can be tackled. It is true that nanomaterials are not dangerous but there is always a chance of scientific uncertainty.

I wish to thank all the authors for their contributions for this book and it is my pleasure to acknowledge the assistance of the publication team throughout the editing process of this book and its preparation in final format. Finally I would like to acknowledge my family who has supported me at every step.

**Editor**



# Contents

---

	<b>Preface</b>	<b>IX</b>
Chapter 1	<b>A Facile Nanodelivery Platform Based on Functionalized Hyperbranched Poly(ether-ester) for Individualized Antitumor Drugs: Pingyangmycin as a Model</b> Xing-ai Jin, Yan-wu Li, Guo-lin Li, Shao-hua Lv, Ying-qun Liu and Li-min Mao	<b>1</b>
Chapter 2	<b>Improving the Osteoblast Cell Adhesion on Electron Beam Controlled TiO<sub>2</sub> Nanotubes</b> Sung Wook Yoon, Hyun Ju Shim and In-Bo Shim	<b>11</b>
Chapter 3	<b>CLSVOF Method to Study the Formation Process of Taylor Cone in Crater-Like Electrospinning of Nanofibers</b> Yong Liu, Jia Li, Yu Tian, Xia Yu, Jian Liu and Bao-Ming Zhou	<b>18</b>
Chapter 4	<b>Preparation and Application of Conductive Textile Coatings Filled with Honeycomb Structured Carbon Nanotubes</b> Filip Govaert and Myriam Vanneste	<b>30</b>
Chapter 5	<b>Thermal Resistance across Interfaces Comprising Dimensionally Mismatched Carbon Nanotube-Graphene Junctions in 3D Carbon Nanomaterials</b> Jungkyu Park and Vikas Prakash	<b>36</b>
Chapter 6	<b>The Effect of Surfactants on the Diameter and Morphology of Electrospun Ultrafine Nanofiber</b> Jian-Yi Zheng, Ming-Feng Zhuang, Zhao-Jie Yu, Gao-Feng Zheng, Yang Zhao, Han Wang and Dao-Heng Sun	<b>46</b>
Chapter 7	<b>Thermal Effect on the Structural, Electrical, and Optical Properties of In-Line Sputtered Aluminum Doped Zinc Oxide Films Explored with Thermal Desorption Spectroscopy</b> Shang-Chou Chang, Tien-Chai Lin and To-Sing Li	<b>55</b>
Chapter 8	<b>Fabrication of Phase-Change Polymer Colloidal Photonic Crystals</b> Tianyi Zhao, Youzhuan Zhang, Jingxia Wang, Yanlin Song and Lei Jiang	<b>61</b>
Chapter 9	<b>Electrohydrodynamic Direct-Write Orderly Micro/Nanofibrous Structure on Flexible Insulating Substrate</b> Jiang-Yi Zheng, Hai-Yan Liu, Xiang Wang, Yang Zhao, Wei-Wei Huang, Gao-Feng Zheng and Dao-Heng Sun	<b>68</b>



Chapter 10	<b>Enhanced Performance of Dye-Sensitized Solar Cells with Graphene/ZnO Nanoparticles Bilayer Structure</b> Chih-Hung Hsu, Cheng-Chih Lai, Lung-Chien Chen and Po-Shun Chan	75
Chapter 11	<b>The Si Nanocrystal Trap Center Studied by Deep Level Transient Spectroscopy (DLTS)</b> Tiezheng Lv and Lili Zhao	81
Chapter 12	<b>Physicochemical Properties of Gold Nanostructures Deposited on Glass</b> Zdenka Novotna, Alena Reznickova, Linda Viererblova, Jiri Kolafa, Zdenka Kolska, Jan Riha and Vaclav Svorcik	87
Chapter 13	<b>Physical-Statistical Model of Thermal Conductivity of Nanofluids</b> B. Usowicz, J. B. Usowicz and L. B. Usowicz	95
Chapter 14	<b>Carrier Statistics and Quantum Capacitance Models of Graphene Nanoscroll</b> M. Khaledian, Razali Ismail, M. Saeidmanesh, M. T. Ahmadi, and E. Akbari	101
Chapter 15	<b>Structural and Electrical Properties of the YSZ/STO/YSZ Heterostructure</b> Yue Fan, Wende Liu, Zhenfeng Kang, Tiezhu Ding, Qingrui Bo, Lingling Xiao, Xiaobing Bai, Pingping Zheng and Qiang Li	107
Chapter 16	<b>High Cycling Performance Cathode Material: Interconnected LiFePO<sub>4</sub>/Carbon Nanoparticles Fabricated by Sol-Gel Method</b> Zhigao Yang and Shengping Wang	112
Chapter 17	<b>Tungsten Oxide and Polyaniline Composite Fabricated by Surfactant-Templated Electrodeposition and Its Use in Supercapacitors</b> Benxue Zou, Shengchen Gong, Yan Wang and Xiaoxia Liu	119
Chapter 18	<b>Label-Free Dengue Detection Utilizing PNA/DNA Hybridization Based on the Aggregation Process of Unmodified Gold Nanoparticles</b> Samsulida Abdul Rahman, Rafidah Saadun, Nur Ellina Azmi, Nurhayati Ariffin, Jaafar Abdullah, Nor Azah Yusof, Hamidah Sidek and Reza Hajian	128
Chapter 19	<b>Photoluminescence of MoS<sub>2</sub> Prepared by Effective Grinding-Assisted Sonication Exfoliation</b> Jing-Yuan Wu, Meng-Na Lin, Long-De Wang and Tong Zhang	133
Chapter 20	<b>Design and Characterization of Electrospun Polyamide Nanofiber Media for Air Filtration Applications</b> Jonas Matulevicius, Linas Kliucininkas, Dainius Martuzevicius, Edvinas Krugly, Martynas Tichonovas and Jonas Baltrusaitis	140

Chapter 21	<b>The Fabrication and Properties Characterization of Wood-Based Flame Retardant Composites</b>	153
	Xia He, Xianjun Li, Zhu Zhong, Yongli Yan, Qunying Mou, Chunhua Yao and Chun Wang	
Chapter 22	<b>Upconversion luminescence and Visible-Infrared Properties of <math>\beta</math>-NaLuF<sub>4</sub>:Er<sup>3+</sup> Microcrystals Synthesized by the Surfactant-Assisted Hydrothermal Method</b>	159
	Han Lin, Xiaohong Yan, Jin Zheng, Changjie Dai and Yuan Chen	
Chapter 23	<b>Enhancing Color Purity and Stable Efficiency of White Organic Light Diodes by Using Hole-Blocking Layer</b>	170
	Chien-Jung Huang, Kan-Lin Chen, Dei-Wei Chou, Yu-Chen Lee and Chih-Chieh Kang	
Chapter 24	<b>A New Method for Superresolution Image Reconstruction Based on Surveying Adjustment</b>	176
	Jianjun Zhu, Cui Zhou, Donghao Fan and Jinghong Zhou	

#### Permissions

#### List of Contributors



# A Facile Nanodelivery Platform Based on Functionalized Hyperbranched Poly(ether-ester) for Individualized Antitumor Drugs: Pingyangmycin as a Model

Xing-ai Jin,<sup>1</sup> Yan-wu Li,<sup>2</sup> Guo-lin Li,<sup>3,4</sup> Shao-hua Lv,<sup>3,4</sup> Ying-qun Liu,<sup>1</sup> and Li-min Mao<sup>3</sup>

<sup>1</sup> Department of Pediatrics, College of Stomatology, Harbin Medical University, 23 Youzheng Street, Harbin 150001, China

<sup>2</sup> Department of Periodontology, College of Stomatology, Harbin Medical University, 23 Youzheng Street, Harbin 150001, China

<sup>3</sup> Department of Oral and Maxillofacial Surgery, College of Stomatology, Harbin Medical University, 23 Youzheng Street, Harbin 150001, China

<sup>4</sup> State Key Laboratory of Metal Matrix Composites, School of Chemistry and Chemical Engineering, Shanghai Jiao Tong University, 800 Dongchuan Road, Shanghai 200240, China

Correspondence should be addressed to Li-min Mao; hrbmlm@126.com

Academic Editor: In-Kyu Park

Nanodelivery of antitumor drugs is a new treatment mode for cancer. The aim of this investigation was to construct and evaluate a facile nanodelivery platform for individualized antitumor drugs based on functionalized hyperbranched poly(ether-ester)s. Poly(ether-ester)s, as a kind of hyperbranched polymers, have received extensive attention. Three terminal-functionalized (OH-, NH<sub>2</sub>- and COOH-) hyperbranched poly(ether-ester)s were prepared and characterized by dynamic light scattering and attenuated total reflectance Fourier transform infrared spectroscopy. The relationship between chemical terminal variation and physical surface charges was investigated. Biocompatibility of these polymers was confirmed by methyl tetrazolium assays and scanning electron microscopy. As a model drug, pingyangmycin has antitumor and antiangiogenic effects. In the paper, pingyangmycin was mixed with carboxyl-modified hyperbranched poly(ether-ester) through ionic binding. Polymer-mixed pingyangmycin exhibited significant inhibition of HN-6 head and neck cancer human cells *in vitro*. These studies demonstrate that functionalized hyperbranched (ether-ester)s can be exploited as a facile nanodelivery platform for antitumor therapy.

## 1. Introduction

Although nanodelivery of antitumor drugs has numerous advantages, such as improved solubility [1], accurate targeting [2–5], increased permeability of tumor vasculature to macromolecules, and decreased lymphatic drainage from the tumor; the complicated techniques involved in nanodelivery development have impeded individualized nanodelivery of numerous antitumor drugs. Even dendritic polymers, which have been used for nanodelivery for years, involve complicated techniques and high costs associated with the crystal architecture [6, 7].

Over the past two decades hyperbranched polymers have received a great deal of attention [8–10]. Since the first intentional preparation of hyperbranched polymers, many types have been synthesized, including polyimide, polyether, poly-

methacrylate, polyphenylene, poly(ether ketone), polyester, and polyurethane [11]. As a novel generation of dendritic polymers, hyperbranched polymers (HBP), which have characteristic incomplete branching and irregular dimensions, provide a facile substitute for the preparation and screening of nanocarriers. Distinct from their linear analogues, hyperbranched polymers have structures and topologies similar to dendrimers and possess some strikingly superior material properties [9, 10]. Due to their low dispersity and excellent biocompatibility and biodegradability [1, 12–16] hyperbranched polymers have been applied in the field of pharmaceutical delivery. In our previous studies, hyperbranched poly(ether-ester) (HPPEE) was prepared, characterized [17, 18], and applied as a nanocarrier of antitumor drug [1, 19]. In the present study, a series of terminal-functionalized derivatives were established based on the HPPEE backbone, thus



providing a facile platform for optimization of individualized antitumor drug delivery. Pingyangmycin is a water-soluble glycopeptide produced by *Streptomyces pingyangensis*. It is chemically similar to bleomycin with antitumor and antiangiogenic effects. In this paper pingyangmycin is used as an example to assess the efficacy of this nanodelivery platform.

## 2. Materials and Methods

**2.1. Synthesis of End-Functionalized HPEE Derivatives.** A suspension of potassium hydride (KH, Aldrich) in mineral oil (30% in weight) was placed in a dry preweighed 100 mL Schlenk flask under nitrogen. The mineral oil was removed by three extractions with tetrahydrofuran (THF), which was added to the flask by syringe. Completely dried KH (0.58 g, 14.46 mmol) was added to 40 mL dimethyl sulfoxide (DMSO) and tetra (ethylene glycol) (TTEG; 5.62 g, 28.92 mmol) (Aldrich, ShangHai). The solution was stirred for 30 min to form the alcoholate potassium. Subsequently, glycidyl methacrylate (GMA; 4.12 g, 29.98 mmol) (Sigma, USA) was added and polymerization was conducted for 24 h at 80°C. The resultant mixture was precipitated in 1000 mL of acetone/diethyl ether (v/v1/4) and then redissolved in methanol and neutralized by filtration over cation-exchange resin. The polymer was precipitated twice from methanol solution into cold diethyl ether and subsequently dried under vacuum at 50°C for 24 h. The purified HPEE-OH was obtained as a highly viscous polymer. For HPEE-NH<sub>2</sub> synthesis, 2 g of HPEE-OH was dissolved into 25 mL of DMF. Fmoc-glycine (2.97 g, 10 mmol), dicyclohexylcarbodiimide (DCC; 4.13 g, 20 mmol), 4-dimethylaminopyridine (DMAP; 0.61 g, 5 mmol), and hydration p-toluene sulfonic acid (PTSA; 0.95 g, 5 mmol) were added to the solution. The mixture was dissolved in 20% piperidine to remove fmoc-protected groups. For HPEE-COOH synthesis, 1 g HPEE-OH was dissolved in 15 mL dichloromethane (CH<sub>2</sub>Cl<sub>2</sub>) under moderate stirring at room temperature. When it was completely dissolved, 1 g of succinic anhydride and 360  $\mu$ L dried piperidine were added to the flask under the same conditions. For comparison and confirmation purposes, the nonbiodegradable structural analogue hyper-branched poly(ether) (HPE) and its functionalized derivatives were concurrently synthesized and analyzed (details are provided in Supplementary Material available online at <http://dx.doi.org/10.1155/2014/601272>). The same synthesis protocols were used for preparation of HPE and its functionalized derivatives.

**2.2. Characterization.** Nuclear magnetic resonance (NMR): <sup>1</sup>H NMR spectra of the polymers were recorded on an Advanced III 400 M spectrometer (Bruker, Germany) in D<sub>2</sub>O as the solvent. Fourier infrared spectra were measured on an EQUINOX55 (Bruker, Germany). Respective potentials were tested using NaCl titrant (25°C, 100 mmol/L, pH = 7) on Malvern Instruments Zetasizer 2000. Dynamic light scattering (DLS) was assessed on Zetasizer Nano S (Malvern Instruments Ltd., Malvern, Worcestershire, UK) at 25°C.

**2.3. Cell Cultures.** NIH/3T3 normal cells (a mouse embryonic fibroblast cell line) were cultured in DMEM supplemented with 10% FBS and antibiotics (50 units/mL penicillin and

50 units/mL streptomycin) at 37°C in a humidified atmosphere containing 5% CO<sub>2</sub>. After 48 h logarithmic growth the attached cells were collected by enzymatic digestion (0.25% pancreatin and 0.02% EDTA) for further assay. HN-6 cancer cells (a human head and neck squamous carcinoma cell line) were cultured in PRMI-1640 supplemented with 10% FBS and antibiotics (200 units/mL penicillin and 50 units/mL streptomycin) at 37°C in a humidified atmosphere containing 5% CO<sub>2</sub>. Using enzymatic digestion (0.25% pancreatin and 0.02% EDTA), cells were passaged with a 1:3 ratio every 2-3 days for numerous cell generations.

**2.4. In Vitro MTT Assay for Cytotoxicity Assessment.** *In vitro* cytotoxicity of a serial dilution of polymer solution against NIH/3T3 cells was measured by the MTT viability assay. Synthesized HPEE-OH, HPEE-NH<sub>2</sub>, and HPEE-COOH were compared with their structural analogues (HPE-OH, HPE-NH<sub>2</sub>, and HPE-COOH). All solutions were dissolved in PBS with serial dilutions of 0.001 mg/mL, 0.01 mg/mL, 0.1 mg/mL, 1 mg/mL, and 10 mg/mL. The same concentration series of dextran and PEI were also prepared as negative and positive controls, respectively. NIH/3T3 cells were seeded into 96-well plates at a seeding density of  $4.0 \times 10^3$  cells per well in 50  $\mu$ L. After 24 h of incubation, the culture medium was removed and replaced with 50  $\mu$ L polymer solution at different concentrations. After treatment with polymers for 24 h, 48 h, and 96 h, 20  $\mu$ L of 5 mg/mL MTT stock solution in PBS was added to each well. After addition of 200  $\mu$ L DMSO to each well and shaking for 5–10 min, the absorbance was measured at a wavelength of 490 nm using BioTek SynergyH4. Cytotoxicity was determined by the absorbance relative to the blank control.

The *in vitro* inhibitory effect of pingyangmycin-mixed polymers against HN-6 cells was also evaluated by MTT assay. After incubation of HN-6 cells ( $8.0 \times 10^3$  cells/well) for 24 h, the culture medium was removed and replaced with 200  $\mu$ L of medium containing pingyangmycin-mixed polymer. Pingyangmycin was tested at serial concentrations of 0.01, 0.1, 1.0, 10, and 100  $\mu$ g/mL.

**2.5. Surface Morphological Features of 3T3 Cells.** 3T3 cells ( $2 \times 10^5$ /mL) were separately cultured with solutions of three end-modified HPEE derivatives and three end-modified HPE analogues. To strengthen the results, each polymer was tested at low concentration (10  $\mu$ g/mL) and high concentration (1 mg/mL) and the corresponding data were compared. Cells that were simultaneously incubated with HPEE derivatives for 1 h are shown in Figure 4(a) (low concentration subgroup) and Figure 4(b) (high concentration subgroup). At the same time, two control experiments were performed: polyethyleneimine (PEI), an accepted cell toxicant, was used as a positive control and dextran with polymer structure was used as a negative control. Normal 3T3 cells incubated with PBS are also shown as a blank control. Cells of each subgroup were collected and fixed with 2.5% glutaraldehyde for 24 h. Morphological features of the cell surface were observed by scanning electron microscopy (SEM) (FEI Corp. USA).

**2.6. Self-Assembly of Pingyangmycin-Mixed Micelle Preparation.** Based on pingyangmycin's physical and chemical

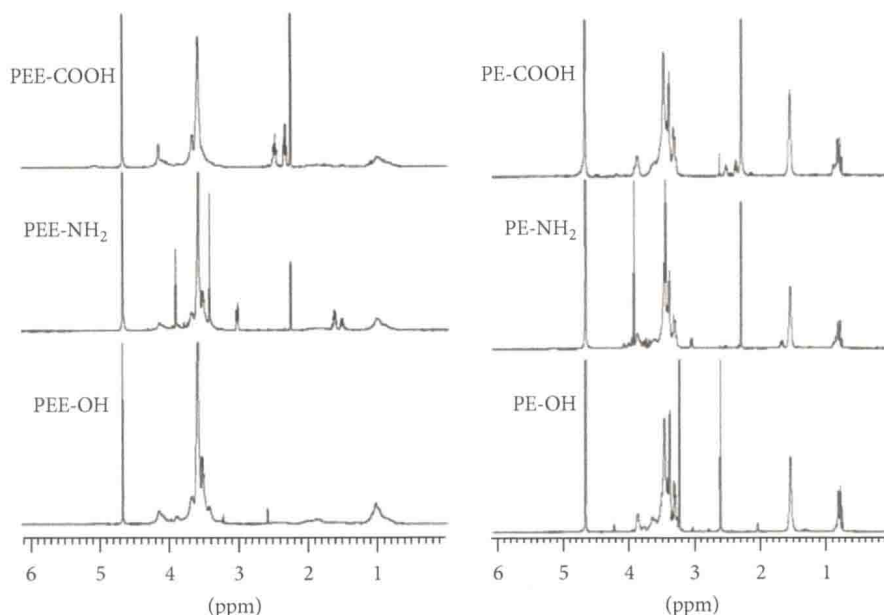


FIGURE 1: Comparison of  $^1\text{H}$  NMR spectra between three PEE-derivatives and three PE-analogues.

characteristics, anionic carboxyl-functionalized HPEE was selected for preparation of micelles. Two functionalized mixtures (HPEE: carboxyl = 1:1 or 1:1.02) were separately added to 10 mL ultrapure water. Pingyangmycin (Bolai Pharmacy Company, China) was then added to each flask with increasing polymer/pingyangmycin ratios of 1:1, 1:2, 1:3, 1:4, and 1:5. All mixtures were stirred at room temperature for 24 h to form a transparent aqueous solution.

**2.7. Visualization of Self-Assembled Micelles by Transmission Electron Microscopy.** Prepared micelle samples that had been dried for 24 h in a vacuum were observed by transmission electron microscopy (TEM) (JEOL2010) at 200 KV.

### 3. Results

**3.1. Synthesis of End-Modified Hyper-Branched Poly(ether-ester)/HPEE Derivatives.** Characterization of the HPEE backbone has been intensively documented in a previous study [20], therefore terminal-modified hyper-branched poly(ether-ester)s could be easily synthesized based on the HPEE backbone according to Scheme 1. Supplemental data address the scheme for preparing structure-matched HPE derivatives.

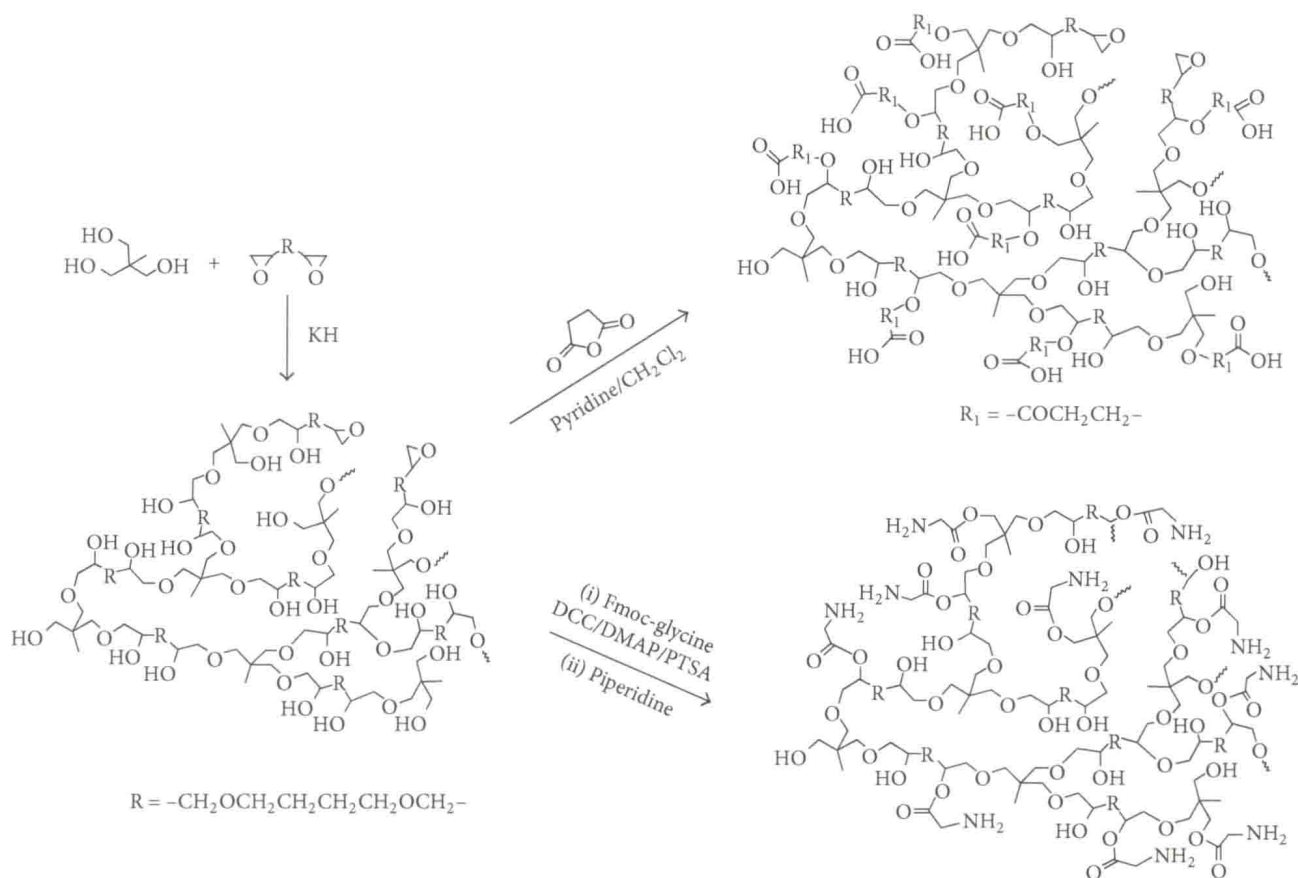
**3.2. Characterization of Functionalized Hyper-Branched Poly(ether-ester)s/HPEE by  $^1\text{H}$  NMR.** According to the quantitative  $^1\text{H}$  NMR spectrum of HPEE (Figure 1, Left), the shift of methyl protons was found to be 1.05 ppm. The backbone of HPEE was observed at 1.80–2.10 ppm and revealed a spectrum of  $-\text{CH}_2-\text{CH}(\text{CH}_2-)-\text{O}-$  or  $-\text{CH}_2-\text{C}(\text{CH}_3)-$  structural subunits. A proton peak of methine adjacent to alcohol oxygen and methylene adjacent to ether oxygen was observed at 4.2–3.3 ppm. Novel peaks could be observed at 2.50 ppm ( $-\text{OCOCH}_2\text{CH}_2\text{COOH}-$ ) and 2.30 ppm ( $-\text{OCOCH}_2\text{CH}_2\text{COOH}-$ ) after the carboxyl

group was grafted onto HPEE. When a glycine residue ( $-\text{OCOCH}_2\text{NH}_2-$ ) was grafted onto HPEE, a novel 3.9 ppm peak that indicated the methylene proton from the amino group could be observed. Similar variation of  $^1\text{H}$  NMR peak-to-terminal could be observed when the same terminals were added to the HPE backbone (Figure 1, Right). The degree of ( $-\text{OCH}_2\text{CH}_2\text{CH}_2\text{CH}_2\text{O}-$ ) in HPE was found to be 1.59 ppm.  $^1\text{H}$  NMR distributions were 0.70–0.85 ppm (hydroxyl protons), 0.70–0.85 ppm (methyl protons), and 3.15–3.70 ppm (methylene and methine adjacent to ether oxygen and alcohol oxygen).

**3.3. Fourier Transform Infrared (FT-IR) Spectra of the Poly(ether-ester) Derivatives.** FT-IR spectra of PEE-OH, PEE-NH<sub>2</sub> and PEE-COOH are shown in Figure 2 (Left). Characteristic ether bond and ester bond absorption bands were shown at  $1100\text{ cm}^{-1}$  and  $1725\text{ cm}^{-1}$ , respectively. A band at  $1668\text{ cm}^{-1}$  could be seen after grafting of amidogen, whereas the  $1557\text{ cm}^{-1}$  band could only be seen after the carboxyl group was grafted. For comparison purposes, FT-R spectra of HPE-analogues are also shown in the same figure (Figure 2, Right). Similarly, the  $1100\text{ cm}^{-1}$  FTIR band in the top HPE-OH figure was produced by asymmetric stretching vibration originating from C–O–C groups. An amidogen absorption band at  $1660\text{ cm}^{-1}$  and a carbonyl absorption band at  $1740\text{ cm}^{-1}$  appeared when  $-\text{NH}_2$  was polymerized into HPE-OH. For HPE-COOH, the carbonyl and carboxyl bands could be observed at  $1730\text{ cm}^{-1}$  and  $1555\text{ cm}^{-1}$ , respectively.

**3.4. Correlation between Surface Potentials and Terminal Groups.** Surface charge varied with chemical terminal functionalization, thus reflecting an interrelationship between physical and chemical variations. As shown in Table 1, the negative potential carried by hydroxyl on the surface of





SCHEME 1: End-functionalization between HPEE and amino group/carboxyl group.

PEE changed to a positive charge when the hydroxyl was replaced by amidogen; conversely, the negative potential of PEE-OH decreased to a more negative value when hydroxyl was replaced by carboxyl. The PE analogues exhibited similar variation in charge-terminal relationships.

**3.5. In Vitro Cytotoxicity against 3T3 Cells.** The results of MTT assays for 3T3 cells following incubation for 24 h, 48 h, and 96 h with various concentrations of the HPEE end-functionalized derivatives are shown in Figure 3. In general, HPEE derivatives demonstrated low cytotoxicity against 3T3 cells. Even 3T3 cells treated with 10 mg/mL HPEE-NH<sub>2</sub>, which was predicted to have the greatest cytotoxicity, for a long incubation time of 96 h retained good viability. The experiment was repeated using the HPE analogues at the same concentrations. Similar MTT results were obtained for HPE-derivatives, as shown in Supplementary Data 2.1.

**3.6. Visualization of 3T3 Cell Surface Morphological Changes by SEM.** Cell surface morphological features were visualized by scanning electron microscopy (SEM). As shown in Figure 4, we observed an extraordinarily smooth surface in normal 3T3 cells, except for a scattering of microvilli and some ruffles at the ends of the pseudopodia. Compared with PBS controls, cells treated with hyperbranched polymers showed notable changes in scattered microvilli and irregular ruffle distributions on cell surfaces that reflected mild adaptation rather than cell injury. None of the cell membranes

lost their integrity during the whole incubation period. As a positive control, severely damaged 3T3 cells cultured in a high concentration of PEI totally lost their fibroblastic shape and the surface topography appeared to be very irregular and destroyed. Similar SEM observations of HPE-derivatives are shown in Supplementary Data 2.1.

**3.7. Self-Assembly of Pingyangmycin into Functionalized HPEE.** To verify the nanocarrier platform based on HPEE functionalized derivants for individualized antitumor drug delivery, we used pingyangmycin as a model drug. Based on the physical and chemical characteristics of pingyangmycin, carboxyl-terminated hyperbranched poly(ether-ester) was selected for bioconjugation as shown in Scheme 2.

After screening, the self-assembly protocol was performed. As shown in Figure 5 and Figure 6, successfully conjugated spherical micelles (Sample 3 and Sample 5) with average diameters of  $156 \pm 9.6$  nm (Sample 3/S3) and  $173 \pm 12.4$  nm (Sample 5/S5) were observed by DLS and TEM visualization.

**3.8. In Vitro Cytotoxicity of Carboxyl-HPEE-Pingyangmycin Micelles against HN-6 Cells.** To evaluate the potential therapeutic efficiency of the carboxyl-terminal-HPEE-pingyangmycin nanocarrier, an *in vitro* MTT assay was performed using HN6 human neck and head carcinoma cells. Both carboxyl-terminated-HPEE-pingyangmycin nanocarriers (S3 and S5) displayed concentration-dependent and time-dependent cytotoxicity as shown in Figure 7. For 24 h

TABLE 1: Correlation between surface potential and end-functionalized polymers.

Delivery vehicle (PEE)	Potential	Comparable analogue (PE)	Potential
PEE-OH	$2.1 \pm 1.2$	PE-OH	$-1.3 \pm 1.1$
PEE-NH <sub>2</sub>	$5.4 \pm 2.5$	PE-NH <sub>2</sub>	$4.2 \pm 0.8$
PEE-COOH	$-11.8 \pm 3.5$	PE-COOH	$-11.7 \pm 2.2$

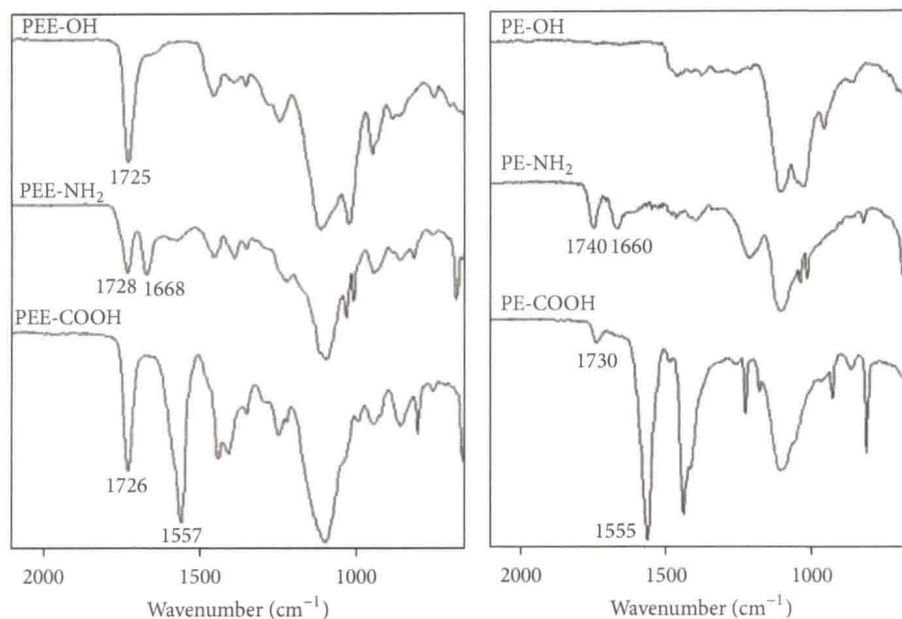


FIGURE 2: Comparison of FT-IR spectra between three PEE-derivatives and three PE-analogues.

treatment, cell viabilities were decreased by 25% for both pingyangmycin alone and pingyangmycin-nanocarrier complexes at concentrations of 0.1 mg/mL to 1 mg/mL. As the concentration increased to 100 mg/mL, cell viabilities significantly reduced. When the time of treatment extended to 48 h, the viability of HN-6 cells was slightly lower than that observed for 24 h treatment.

#### 4. Discussion

Theoretically, a facile platform could be constructed using functionalized hyperbranched polymer derivatives such that a series of nanocarriers could be obtained for optimization of individualized antitumor-drug delivery. Hyperbranched polymers are characterized by three-dimensional cavities with abundant surface terminals and therefore represent an ideal candidate backbone [1, 21–23]. As shown in Scheme 1, ion-transfer polymerization was observed during HPEE terminal functionalization. A hydroxyl group initially reacted with butanedioic anhydride to form a carboxyl group [24, 25]. The carboxyl end then reacted with the glycine that was protected by the 9-carbonyl methoxycarbonyl group to generate an amino group by subsequent esterification [26], after which methoxycarbonyl protection was rapidly removed. Using the facile polymerization procedure presented here, a series of terminal-functionalized polymers were simultaneously prepared. Subsequent studies revealed physical-chemical interrelationships during functionalization. For

confirmation purposes, HPEEs and their HPE structural analogues were simultaneously observed. The similar results confirmed a correlation between physical surface charge and chemical terminal structure; thus, tunable modification of physical charges could be easily achieved by chemical functionalization. Based on this physical-chemical correlation, a tunable nanodelivery platform based on a functionalized HPEE backbone was initially constructed for individualized antitumor drug delivery.

Although good biocompatibility of hyperbranched polymers has been reported [27], the potential cytotoxicity of functionalized HPEE has not been documented. According to the MTT assays, all HPEE derivatives demonstrated excellent biocompatibility even when high concentrations of polymers were used. Furthermore, the biocompatibility of end-modified HPEEs was confirmed by SEM visualization. Previous studies have found that cationic charge of polymers was one of the risk factors for increased cytotoxicity. Due to complicated mechanisms including interactions between cell membranes [28], generation-related clearance [29], and inherent toxicity [30], a strong positive charge of primary amino groups significantly increased the cytotoxicity [28]. Overall, the greatest cytotoxicity of the entire platform was indeed observed for high concentrations of the HPE-NH<sub>2</sub> subgroup, consistent with the previous study. Similarly, mildly enhanced cytotoxicity was observed when the ionic HPEE-COOH subgroup was substituted by the cationic HPEE-NH<sub>2</sub> subgroup. However, relatively good biocompatibility was demonstrated for all HPEE-derivatives in the plat-



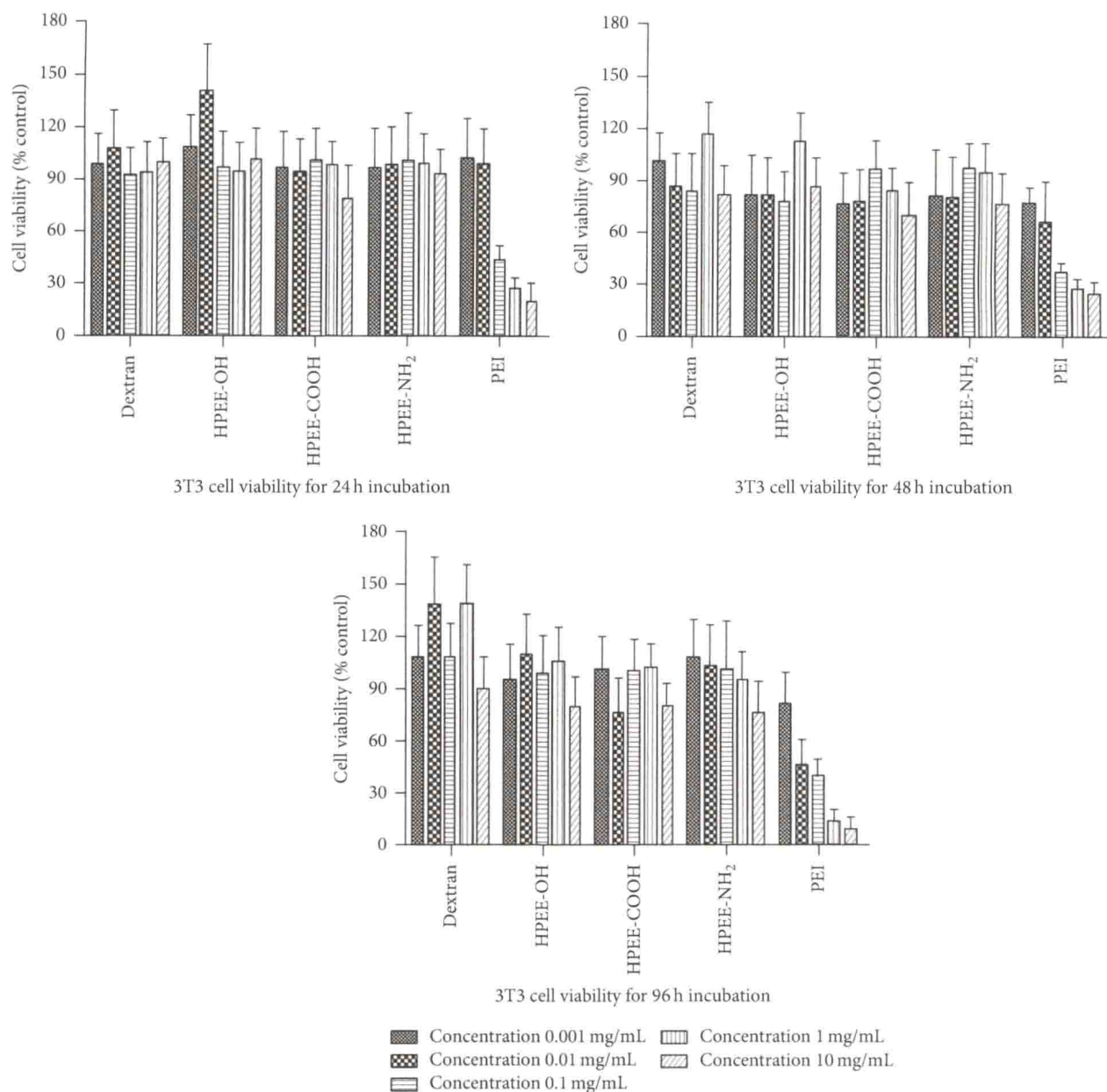


FIGURE 3: 3T3 cell viability following treatment with various concentrations of HPEE-derivatives.

form, including cationic HPEE derivatives despite previous reports of time- and concentration-dependent cytotoxicity of cationic polymers [28]. The mechanism of the reduced cytotoxicity of cationic HPEE functionalization was attributed to scattered surface charge density and the unique uncompleted hyperbranched architecture.

To evaluate potential application of the present nanodelivery platform, an anticancer drug, pingyangmycin (Bleomycin A5), was used as a model agent to assess assembly capability. Pingyangmycin is an antibiotic that was initially isolated from the culture medium of *Streptomyces pingyangensis* spp. in China and has been known for a long time to exhibit significant cytotoxicity to tumor cells [31–34]. Despite its effective antitumor activity, the systemic toxicity and short half-life time of pingyangmycin have largely prevented its widespread clinical application. Therefore, hydrophilic

pingyangmycin has only been used *in situ* to treat head and neck cancers [31–34]. The specific benefits of nanocarriers, such as passive and accurate targeted therapy with decreased systemic toxicity and long circulation [16], could increase the clinical application of pingyangmycin. As shown in Scheme 2, taking into account the amino-bonding surface of pingyangmycin, electrostatic interactions would theoretically be formed between the positive-charged protonated amines of pingyangmycin and the surface carboxyl groups on the oxidized HPEE [35]; therefore, a self-assembled micelle could potentially be constructed in water. Although it is well documented that hyperbranched polymers possess great capability for self-assembly in solution, the issue of interfacial self-assembly and hybrid self-assembly [18, 36–38] and whether and how functionalized HPEE could successfully mix with pingyangmycin was unknown. In addition, some properties